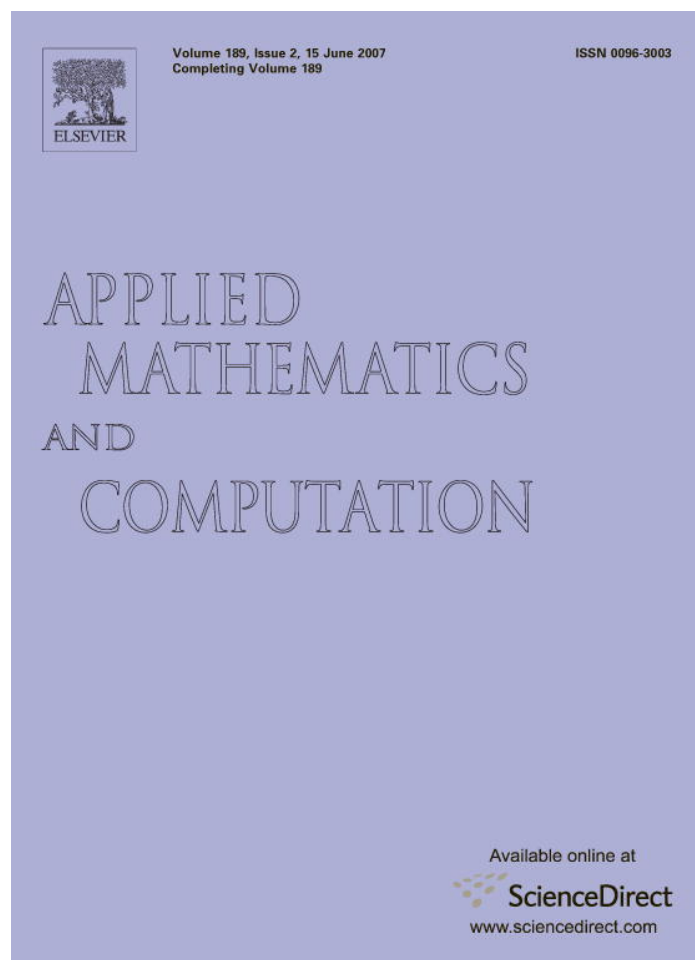


Provided for non-commercial research and educational use only.
Not for reproduction or distribution or commercial use.



This article was originally published in a journal published by Elsevier, and the attached copy is provided by Elsevier for the author's benefit and for the benefit of the author's institution, for non-commercial research and educational use including without limitation use in instruction at your institution, sending it to specific colleagues that you know, and providing a copy to your institution's administrator.

All other uses, reproduction and distribution, including without limitation commercial reprints, selling or licensing copies or access, or posting on open internet sites, your personal or institution's website or repository, are prohibited. For exceptions, permission may be sought for such use through Elsevier's permissions site at:

<http://www.elsevier.com/locate/permissionusematerial>



ELSEVIER

Available online at www.sciencedirect.com

 ScienceDirect

Applied Mathematics and Computation 189 (2007) 1966–1981

APPLIED
MATHEMATICS
AND
COMPUTATION

www.elsevier.com/locate/amc

Comparison of different numerical Laplace inversion methods for engineering applications

Hassan Hassanzadeh, Mehran Pooladi-Darvish *

Department of Chemical and Petroleum Engineering, University of Calgary, 2500 University Drive NW, Calgary, AB, Canada T2N 1N4

Abstract

Laplace transform is a powerful method for enabling solving differential equation in engineering and science. Using the Laplace transform for solving differential equations, however, sometimes leads to solutions in the Laplace domain that are not readily invertible to the real domain by analytical means. Numerical inversion methods are then used to convert the obtained solution from the Laplace domain into the real domain. Four inversion methods are evaluated in this paper. Several test functions, which arise in engineering applications, are used to evaluate the inversion methods. We also show that each of the inversion methods is accurate for a particular case. This study shows that among all these methods, the Fourier transform inversion technique is the most powerful but also the most computationally expensive. Stehfest's method, which is used in many engineering applications is easy to implement and leads to accurate results for many problems including diffusion-dominated ones and solutions that behave like e^{-t} type functions. However, this method fails to predict e^t type functions or those with an oscillatory response, such as sine and wave functions.

© 2007 Published by Elsevier Inc.

Keywords: Laplace transform; Numerical inversion; Fourier transform; Stehfest's algorithm; Test function

1. Introduction

Laplace transform is an efficient method for solving many differential equations in engineering applications. The main difficulty with Laplace transform method is in inverting the Laplace domain solution into the real domain. Laplace transform of a function $f(t)$ can be expressed as follows [1,2]:

$$F(s) = \int_0^{\infty} e^{-st} f(t) dt, \quad (1)$$

where s is a complex variable known as the Laplace variable. Here and in the following sections, a capital F will represent the function in the Laplace domain, whose inversion in real time, $f(t)$, is required. It is noted that t can be any independent variable. However, in this paper, and because of its association with “time”, in many engineering applications we will call it “time”. The inversion integral is defined as follows [1]:

* Corresponding author.

E-mail address: pooladi@ucalgary.ca (M. Pooladi-Darvish).

Nomenclature

a	constant in the Fourier series method
c	fluid compressibility, $[LT^2/M]$, 1/kPa
erfc	complementary error function
f	time domain function
F	Laplace domain function
k	porous media permeability, $[L^2]$, m^2
K_0	modified Bessel function of order zero
K_1	modified Bessel function of order one
j	$\sqrt{-1}$
J_0	Bessel function of order zero
n	number of terms in inversion algorithm
N	number of individual matrix blocks in a stack
N_{Pe}	Peclet number
p	pressure, $[M/LT^2]$, kPa
p^*	normalized pressure
p_{Df}	dimensionless fracture pressure
\bar{p}_{Df}	dimensionless fracture pressure in Laplace space
q	volumetric flow rate, $[L^3/T]$, m^3/s
Q	normalized flow rate
r_D	dimensionless well bore radius
Re	real part of a complex number
s	Laplace variable
S_g	gas saturation
\bar{S}_g	gas saturation in Laplace domain
t	time, $[T]$, s
T	normalized time
t_D	dimensionless time
T_D	dimensionless temperature
\bar{T}_D	dimensionless temperature in Laplace space
x	distance from origin, $[L]$, m
x_D	dimensionless length
z_D	dimensionless matrix block height
μ	fluid viscosity, $[M/LT]$, Pa s
ϕ	porosity
ω	fracture storativity
λ	matrix-fracture inter-porosity flow coefficient
γ	a dimensionless constant

$$f(t) = \frac{1}{2\pi j} \int_{\sigma-j\infty}^{\sigma+j\infty} e^{st} F(s) ds, \quad (2)$$

where σ is chosen so that all the singular points of $F(s)$ lie to the left of the line $\text{Re}\{s\} = \sigma$ in the complex s -plane [3].

Sometimes, an analytical inversion of a Laplace domain solution is difficult to obtain; thus, a numerical inversion method must be used. There are several numerical algorithms in literature that can be used to perform the Laplace inversion. Each individual method has its own application and is suitable for a particular type of function. All the inversion methods are based on approximations used to evaluate the integral given in Eq. (2). Several studies have investigated the mathematics behind this integral evaluation that have led to the different numerical inversion methods.

The following sections present formulations for the four frequently used inversion algorithms. Next, these inversion methods are compared against a number of test functions.

2. Stehfest's method

This numerical Laplace inversion technique was first introduced by Graver [4] and its algorithm then offered by Stehfest [5]. This method has been used extensively in petroleum engineering literature [6].

Stehfest's algorithm approximates the time domain solution using the following equation [5,6]:

$$f(t) = \frac{\ln 2}{t} \sum_{i=1}^n V_i F\left(\frac{\ln 2}{t} i\right), \quad (3)$$

where V_i is given by the following equation:

$$V_i = (-1)^{\binom{n}{2}+1} \sum_{k=\binom{i+1}{2}}^{\min\left(i, \frac{n}{2}\right)} \frac{k^{\binom{n}{2}+1} (2k)!}{\left(\frac{n}{2} - k\right)! k! (i - k)! (2k - 1)!}. \quad (4)$$

The parameter n is the number of terms used in the summation in Eq. (3) and should be optimized by trial and error. Increasing n increases the accuracy of the result up to a point, and then the accuracy declines because of increasing round-off errors. An optimal choice of $10 \leq n \leq 14$ has been reported by Lee et al. for some problem of their interest [6]. This method results in accurate solutions when the time function is in the form of e^{-t} . It is very simple to implement, but it leads to inaccurate solutions for some functions.

3. Zakian's method

Zakian's method [7,8] approximates the time domain function using the following infinite series of weighted evaluations of domain function [9]:

$$f(t) = \frac{2}{t} \sum_{i=1}^n \operatorname{Re} \left\{ K_i F\left(\frac{\alpha_i}{t}\right) \right\}. \quad (5)$$

The constants K_i and α_i for $n = 5$ are given in Table 1.

This method is fast and easy to implement, and there is one free parameter, n , to be determined. The parameter n should be optimized to obtain accurate solutions. Zakian's method is suitable for time domain solutions that have a positive exponential term, e^t . The method requires using complex arithmetic. Lee et al. [6] found that an accurate solution is obtained in a well-testing application of single well pulse testing when $n = 10$.

4. Fourier series method

Dubner and Abate [10] were the first to use the Fourier series technique for the Laplace inversion. The technique is based on choosing the contour of integration in the inversion integral, converting the inversion integral into the Fourier transform, and, then, approximating the transform by a Fourier series. This method approximates the inversion integral using the following equation:

Table 1
Five constants for α and K for the Zakian method [10]

i	α	K
1	12.83767675 + j1.666063445	-36902.08210 + j196990.4257
2	12.22613209 + j5.012718792	+61277.02524 - j95408.62551
3	10.93430308 + j8.409673116	-28916.56288 + j18169.18531
4	8.776434715 + j11.92185389	+4655.361138 - j1.901528642
5	5.225453361 + j15.72952905	-118.7414011 - j141.3036911

$$f(t) = \frac{e^{at}}{t} \left\{ \frac{1}{2} F(a) + \operatorname{Re} \sum_{k=1}^n F\left(a + j \frac{k\pi}{t}\right) (-1)^k \right\},$$

where

$$j = \sqrt{-1}. \quad (6)$$

The parameters a and n must be optimized for increased accuracy. Lee et al. [6] suggested values of at between 4 and 5.

5. Schapery's method

Schapery's method [11] is a simple analytical inversion technique that is very simple to implement. It leads to approximate solutions, and therefore is suitable for the initial evaluation of the time domain solution: for example, when the global behaviour of the time domain solution needs to be predicted. Jelmert [12] reported an accuracy of 5% in a petroleum engineering application of linear flow. This method is applicable when the Laplace domain solution is in the form of $sF(s) = As^m$ and $m < 1$. In this case, the following relationship exists between the real time solution and its form in the Laplace domain [12]:

$$f(t) \approx [sF(s)]_{s=\frac{1}{\gamma}}, \quad (7)$$

where $\gamma = 1.781$.

6. Evaluation of different inversion algorithms

In the following section(s), a number of test functions in the Laplace domain are used to examine the accuracy in inverting them into the real domain. In all cases, the numerical solutions are compared against the analytical conversion solution. In addition to a number of test functions often used for studying the accuracy of Laplace inversion techniques, a number of solutions of engineering problems are also considered [6,13,14]. In some cases, where the analytical solution in the real time domain is unavailable, the solutions are compared only with each other.

6.1. Function $f(t) = 1$, $F(s) = \frac{1}{s}$

Fig. 1 shows that all inversion techniques provide an accurate prediction of the real domain solution.

6.2. Function $f(t) = e^{-t}$, $F(s) = \frac{1}{s+1}$

Fig. 2 compares different inversion methods for function 6.2. The Fourier series and the Stehfest algorithm give very accurate results. The Zakian conversion is not as accurate for small time values. Schapery's method provides poor results, especially at late times. Its results are good probably only for a prediction of the global behaviour of the time domain solution.

6.3. Function $f(t) = e^t$, $F(s) = \frac{1}{s-1}$

A comparison between inversion methods is provided in Fig. 3. Results show that Stehfest's algorithm is inaccurate for e^t type functions. In addition, it is clear that Schapery's method fails in this case; however, the trend is preserved in the solution. The Fourier series technique and Zakian's algorithm give accurate results, while the Fourier series technique gives more accurate results than does the Zakian algorithm.

6.4. Function $f(t) = \sin(t)$, $F(s) = \frac{1}{s^2+1}$

Fig. 4 provides a comparison among different inversion methods. The Fourier series method provides an excellent match with the analytical solution. Stehfest's algorithm gives good results in one cycle but then fails.

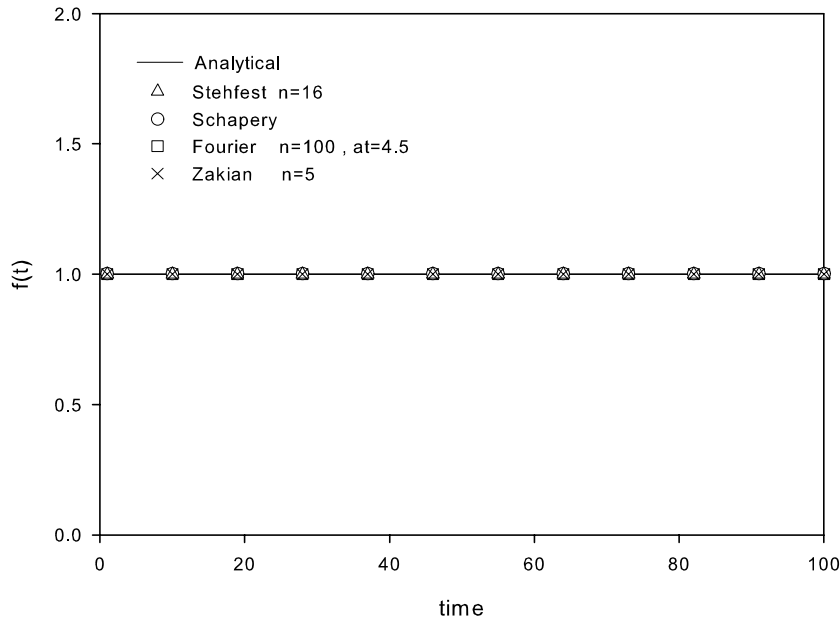


Fig. 1. Comparison of different numerical inversion methods for $f(t) = 1$.

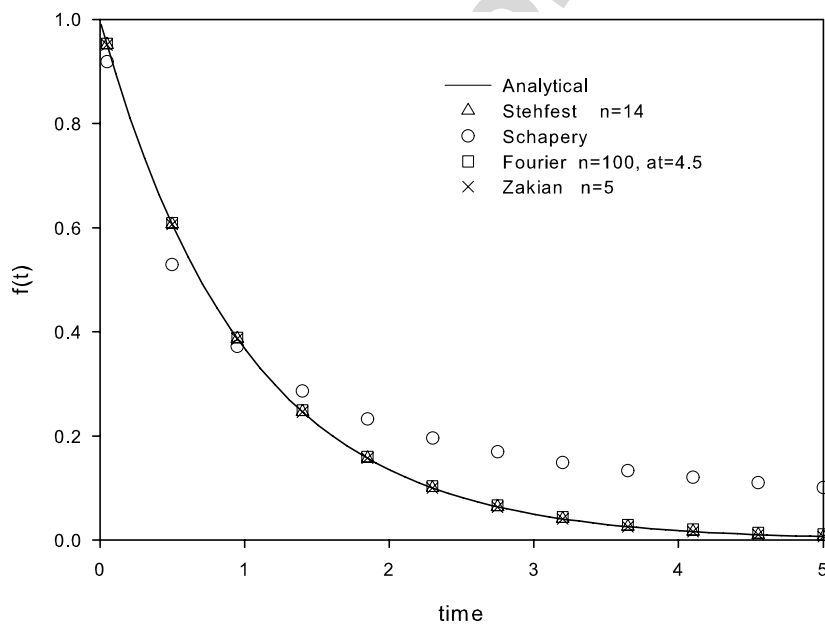


Fig. 2. Comparison of different numerical inversion methods for $f(t) = e^{-t}$.

Figs. 4 and 5 show that Zakian’s method predicts accurately up to three cycles, while Schapery’s method fails completely.

6.5. Function $f(t) = J_0(t)$, $F(s) = \frac{1}{\sqrt{s^2+1}}$

Fig. 6 shows that Stehfest’s algorithm gives accurate results only for early times and fails to predict the late time behavior. Schapery’s method fails entirely. In contrast, the Fourier series and Zakian’s inversion method both give accurate results, with the Fourier series giving more accurate results than Zakian’s method.

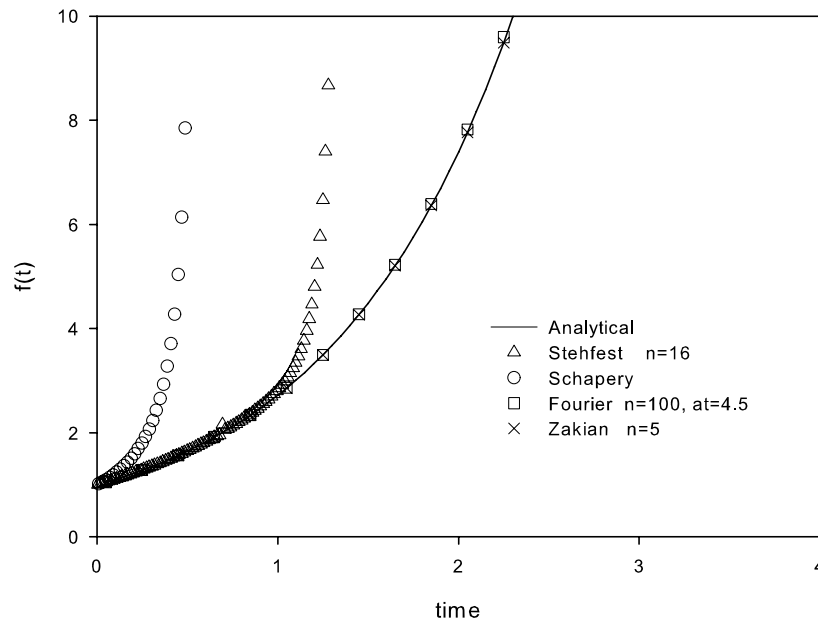


Fig. 3. Comparison of different numerical inversion methods for $f(t) = e^t$.

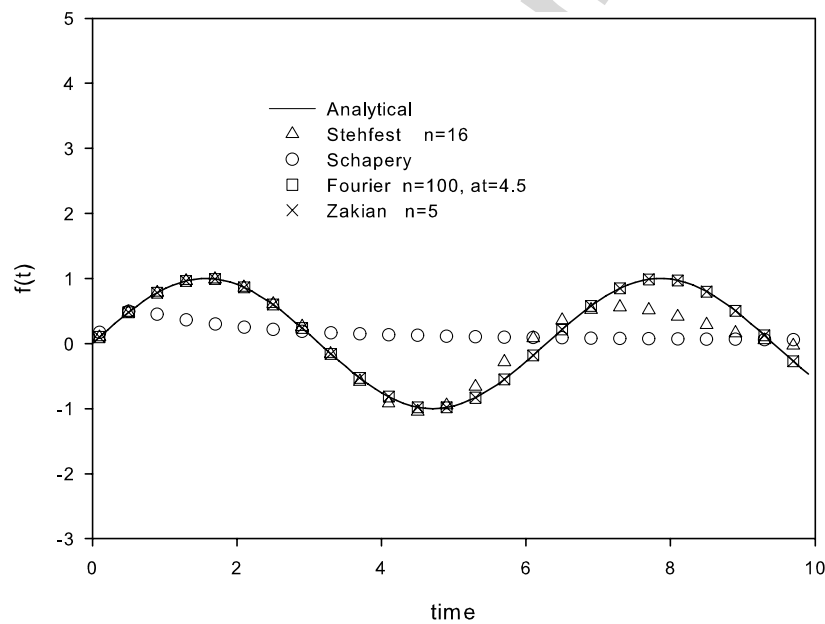


Fig. 4. Comparison of different numerical inversion methods for $f(t) = \sin(t)$.

6.6. Square wave function

Fig. 7 shows a square wave function in time domain. Results for different inversion methods are provided in Fig. 8. Among all the inversion methods studied, only the Fourier series method predicts the square wave function accurately. Both the Zakian and Stehfest algorithms have instability, while Schapery’s method is stable but inaccurate.

6.7. Nonlinear pressure diffusion

The partial differential equation that describe a single-phase flow of a slightly compressible fluid in porous media of constant porosity is non-linear when expressed in terms of pressure and is given by Odeh and Babu [15]

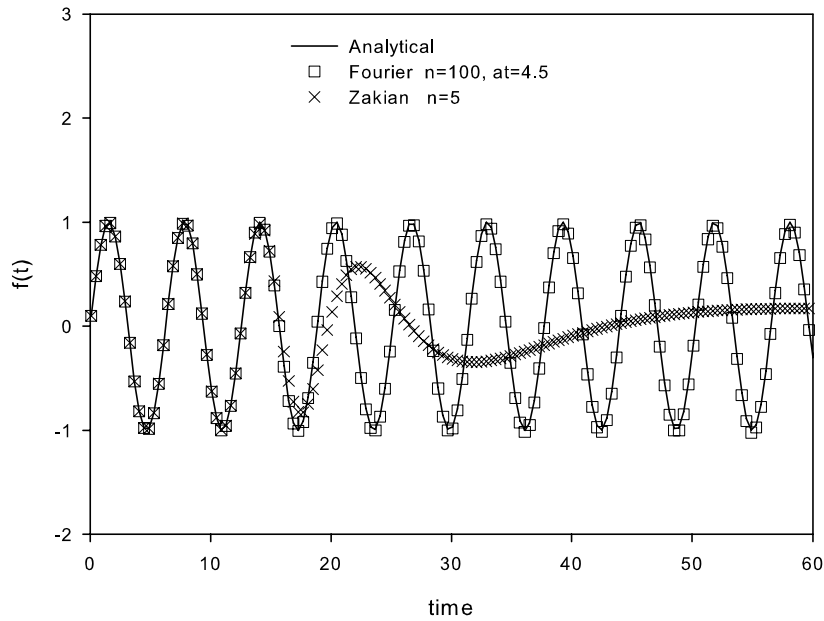


Fig. 5. Comparison of different numerical inversion methods for $f(t) = \sin(t)$.

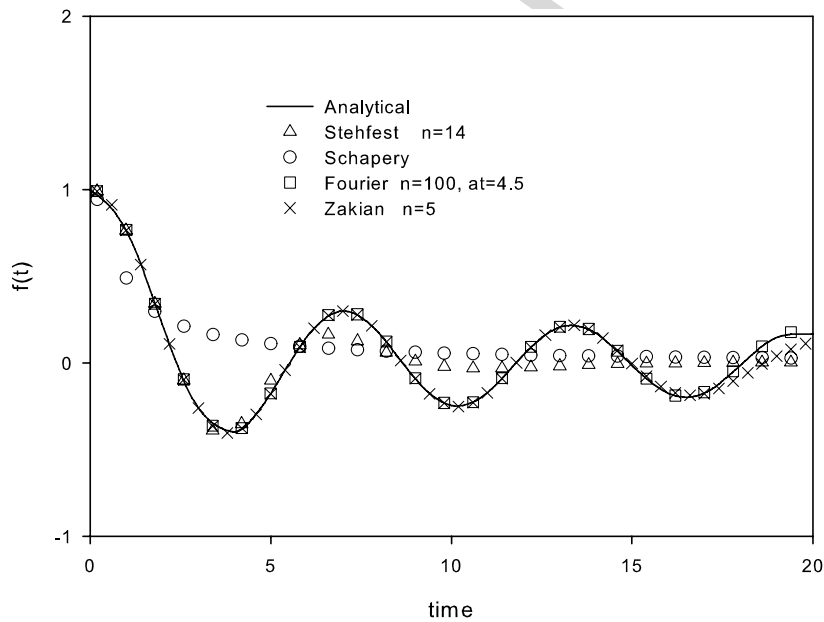


Fig. 6. Comparison of different numerical inversion methods for $f(t) = J_0(t)$.

$$\frac{\partial^2 p}{\partial x^2} + c \left(\frac{\partial p}{\partial x} \right)^2 = \frac{\phi \mu c}{k} \frac{\partial p}{\partial t}. \tag{8}$$

In Eq. (8), p is pressure, x is distance, c is fluid compressibility, ϕ is porosity, μ is viscosity, k is permeability, and t is time in a consistent system of measurement units. For a constant rate production and infinite acting behavior, the initial and boundary conditions are

$$p = p_i \quad \text{at } t = 0,$$

$$\frac{\partial p}{\partial x} = Q \quad \text{where } Q = \frac{q\mu}{kA} \quad \text{at } x = 0,$$

and $p = p_i$ as x goes to infinity.

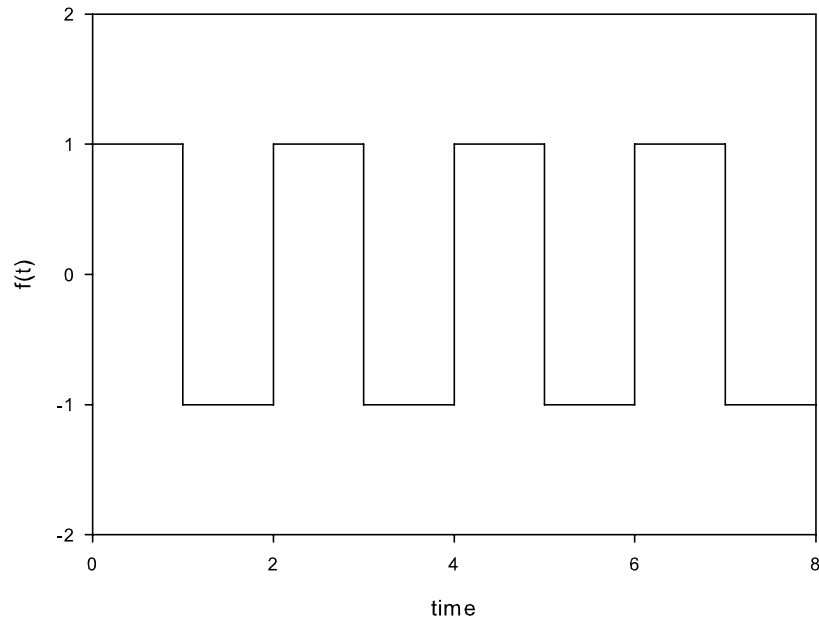


Fig. 7. Square wave function.

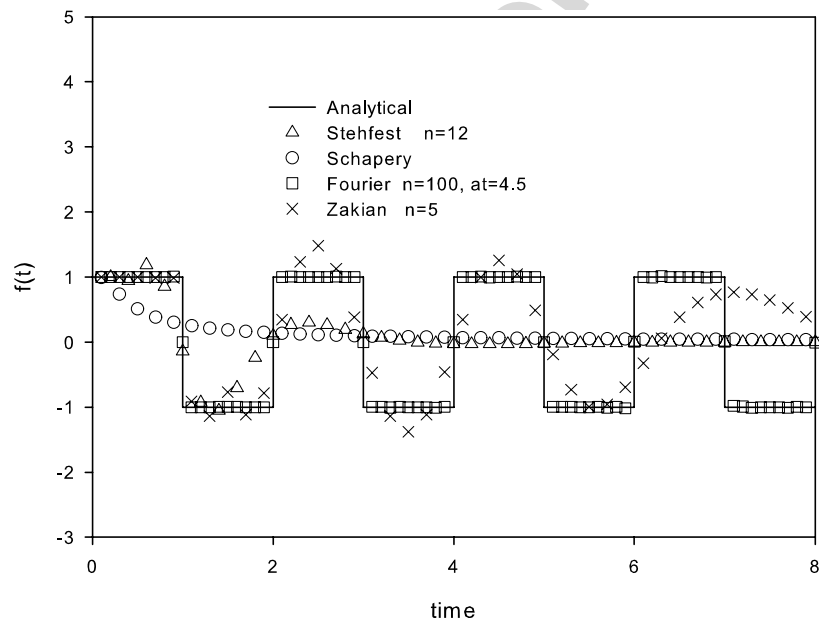


Fig. 8. Comparison of different numerical inversion methods for square wave.

The non-linear PDE can be linearized by the following transformation.

Let $\Delta p = p - p_i$, $T = \frac{kt}{\phi\mu c}$ and $\Delta p = \frac{1}{c} \ln p^*$ then Eq. (8) becomes

$$\frac{\partial^2 p^*}{\partial x^2} = \frac{\partial p^*}{\partial T}. \tag{9}$$

Initial and boundary conditions in the transformed state are

$$p^*(x, 0) = 1 \quad \text{at } T = 0,$$

$$\frac{\partial p^*}{\partial x} = Qcp^* \quad \text{at } x = 0,$$

and

$$p^* \rightarrow 1 \quad \text{as } x \rightarrow \infty.$$

The following equations, respectively, give solutions to Eq. (9) in the Laplace and time domains [15]:

$$\bar{p}^*(x, s) = -\frac{Qc}{s(\sqrt{s} + Qc)} \exp(-x\sqrt{s}) + 1/s, \tag{10}$$

$$p^*(x, T) = e^{Qc(x+QcT)} \operatorname{erfc}\left(Qc\sqrt{T} + \frac{x}{2\sqrt{T}}\right) - \operatorname{erfc}\left(\frac{x}{2\sqrt{T}}\right) + 1, \tag{11}$$

where for the physical properties considered by Odeh and Babu, $Qc = 2.38 \times 10^{-4}$ and $T = 0.05457t$, t is in seconds and x is in feet [15].

Fig. 9 shows a comparison of the different inversion methods. All the inversion methods give an accurate result except Schapery's method.

6.8. Re-infiltration in naturally fractured reservoirs

The gravity drainage process from a stack of N matrix blocks may be described by the following convection–diffusion equation. The underlying assumptions are given by Firoozabadi and Ishimoto [16]

$$\frac{\partial S_g}{\partial t_D} = \frac{\partial}{\partial z_D} \left(\frac{\partial S_g}{\partial z_D} + 2\gamma S_g \right). \tag{12}$$

The initial and boundary conditions for an individual matrix block can be expressed as follows:

$$S_g = 0, \quad t_D = 0, \quad 0 \leq z_D \leq 1,$$

$$2\gamma(1 - S_g) - \frac{\partial S_g}{\partial z_D} = (q_{DI-1})_{z_D=0} \quad \text{at } z_D = 1$$

and

$$S_g = 0 \quad \text{at } z_D = 0.$$

In the equations above, S_g is gas saturation in the matrix block, t_D is dimensionless time, z_D is dimensionless block height, q_D is the dimensionless matrix block re-infiltration rate, and γ is a dimensionless constant.

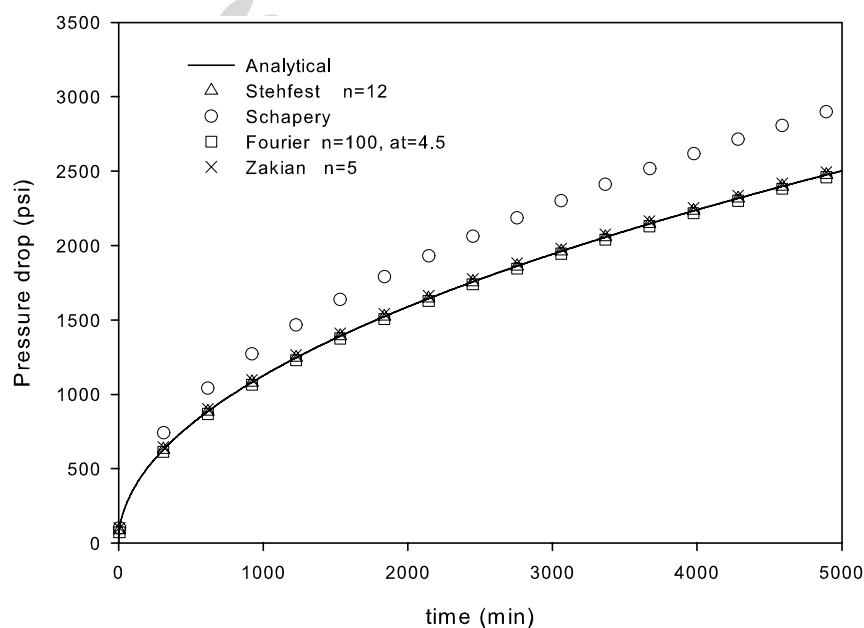


Fig. 9. Comparison of different numerical inversion methods for non-linear diffusion equation.

The Laplace transform yields a general solution for block I, which is given below [16]

$$\bar{S}_g^I = \left(\frac{2\gamma}{s}\right) \left(\frac{e^\gamma}{A}\right)^I (\sqrt{s + \gamma^2})^{I-1} e^{-\gamma z_D} \sinh \left[(\sqrt{\gamma^2 + s}) z_D \right], \tag{13}$$

where

$$A = \left[\gamma \sinh (\sqrt{\gamma^2 + s}) + (\sqrt{\gamma^2 + s}) \cosh (\sqrt{\gamma^2 + s}) \right].$$

The average gas saturation in each block can be obtained by the integration of the saturation equation over each matrix block as given below

$$\bar{S}_{gAVE} = \left(\frac{2\gamma}{s}\right) \left(\frac{e^\gamma}{A}\right)^I (\sqrt{s + \gamma^2})^{I-1} (Ae^{-\gamma} - (\sqrt{s + \gamma^2})), \tag{14}$$

where $\gamma = 0.35$ and I is the block index. In the calculation below, N is assumed to be 10.

Fig. 10 compares the results obtained from different inversion methods for average gas saturation in block number 10. Although no analytical solution is available for comparison, three of the inversion methods give approximately the same results. All the solutions agree except for Schapery's, which is far away from the others.

In comparison to the other three inversion methods, the Fourier series results are without oscillations, and the results are smoother than the other two methods. The Stehfest and Zakian algorithms show very small oscillations in the early and late time solutions, respectively.

6.9. Constant rate solution of diffusivity equation in a fractured reservoir

The following equation gives the differential equation and the associated boundary conditions that describe the pressure diffusion in a naturally fractured reservoir under a pseudo-steady state matrix-fracture transfer in the Laplace domain [17]

$$\frac{d^2 \bar{p}_{Df}}{dr_D^2} + \frac{1}{r_D} \frac{d\bar{p}_{Df}}{dr_D} = sf(s)\bar{p}_{Df}, \tag{15}$$

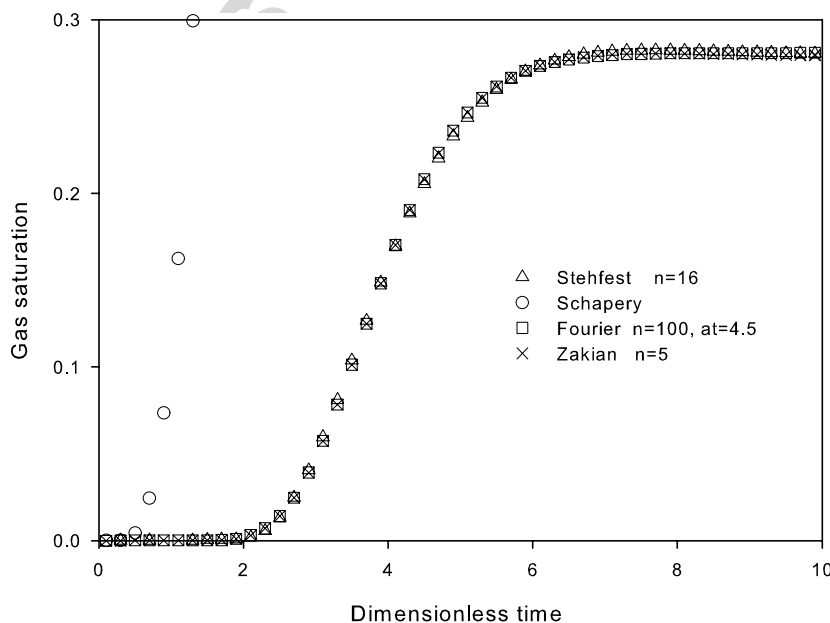


Fig. 10. Comparison of different numerical inversion methods for convection–diffusion equation.

where

$$f(s) = \frac{\omega(1 - \omega)s + \lambda}{(1 - \omega)s + \lambda},$$

$$\bar{p}_{Df} = 0 \quad \text{at } r_D = \infty$$

and

$$\frac{d\bar{p}_{Df}}{dr_D} = -\frac{1}{s} \quad \text{at } r_D = 1,$$

where p_{Df} , ω , and λ are the dimensionless fracture pressure, fracture storativity, and inter-porosity flow coefficient respectively. The constant rate solution of the diffusivity equation for a fractured reservoir subject to the given initial and boundary conditions at the well radius in the Laplace domain can be expressed as [17]

$$\bar{p}_{Df} = \frac{K_0(\sqrt{sf(s)})}{s\sqrt{sf(s)}[K_1(\sqrt{sf(s)})]}. \tag{16}$$

During a well test in a naturally fractured reservoir, when a pressure drop develops between a matrix and a fracture, matrix blocks start to support the fissured system. This phenomenon is characterized by a dip in the derivative curve and is known as a *transition period*. The pressure derivative is defined as $dp_{Df}/d \ln t_D$. This derivative is more sensitive than the pressure when it is plotted against time in a logarithmic scale. In other words, more information can be obtained from a derivative curve than from a pressure curve. In practice, however, pressure and its derivative are plotted together to analyze a well test data.

Eq. (16) is inverted by using different methods; the results are compared in Fig. 11 in terms of pressure and the pressure-derivative function. The results agree well with each other, except for Schapery’s method, which is different from the others in the transition period.

6.10. Mixing model of stirred vessels

A stirred tank model, which is encountered in chemical engineering applications, is selected in this part. For the system reported by Halsted and Brown [9] the Laplace domain response of the mixing model is given by

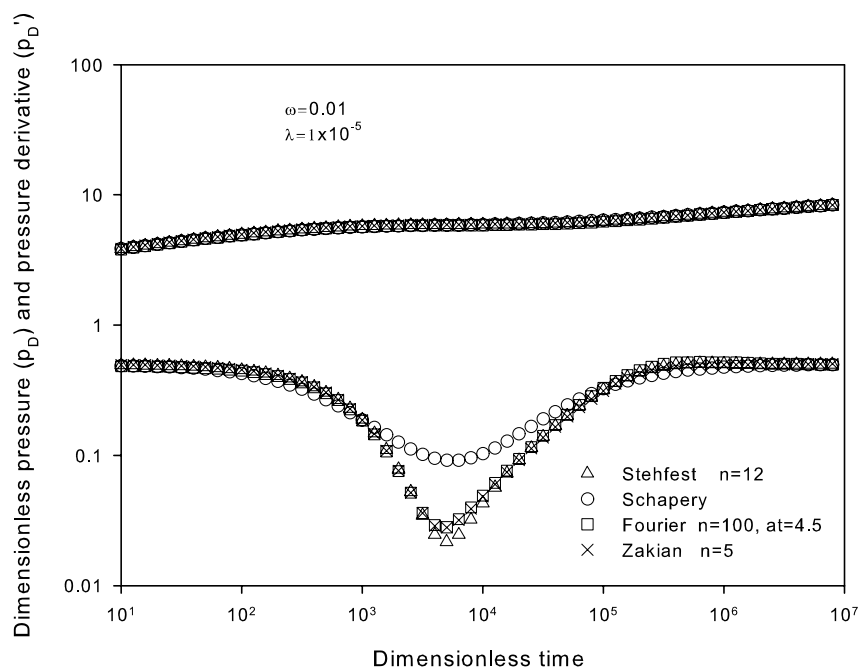


Fig. 11. Comparison of different numerical inversion methods for a double-porosity model.

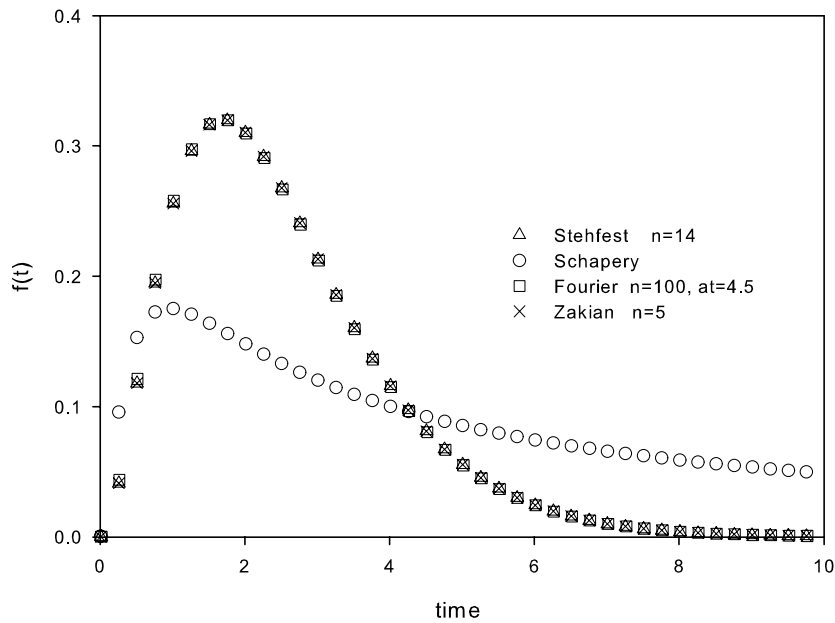


Fig. 12. Comparison of different numerical inversion methods for a stirred vessel.

$$F(s) = \frac{1}{(1 + 0.845s)^3}. \tag{17}$$

Fig. 12 shows a comparison of the four inversion methods. Except for Schapery’s method, all the inversion methods result in almost the same time domain response.

6.11. Heat conduction

The partial differential equation that describes heat conduction in a solid of dimensionless length 2, which is initially at a unit dimensionless temperature and suddenly brought to zero on both side, may be described by the following equation [14]:

$$\begin{aligned} \frac{\partial^2 T_D}{\partial x_D^2} &= \frac{\partial T_D}{\partial t_D}, \\ T_D(x, 0) &= 1, \\ T_D(-1, t_D) &= 0, \\ T_D(1, t_D) &= 0, \end{aligned} \tag{18}$$

where T_D is temperature, x_D is length and t_D is time all in dimensionless form.

The analytical solution to this equation is given by

$$T_D(x_D, t_D) = \frac{4}{\pi} \sum_0^\infty \frac{(-1)^n}{2n + 1} \exp\left(-\frac{(2n + 1)^2 \pi^2 t_D}{4}\right) \cos\left(\frac{(2n + 1)\pi x_D}{2}\right). \tag{19}$$

The solution to Eq. (18) in the Laplace domain can be expressed as [14]

$$\bar{T}_D(x_D, s) = \frac{1}{s} \left(1 - \frac{\cosh \sqrt{sx_D}}{\cosh \sqrt{s}}\right). \tag{20}$$

This equation is inverted numerically by different inversion methods. The results obtained from the different inversion methods and the analytical solution are given in Figs. 13 and 14. In all cases except one, the results agree well with the analytical solution. Schapery’s method is not accurate, but it does predict the solution’s global trend.

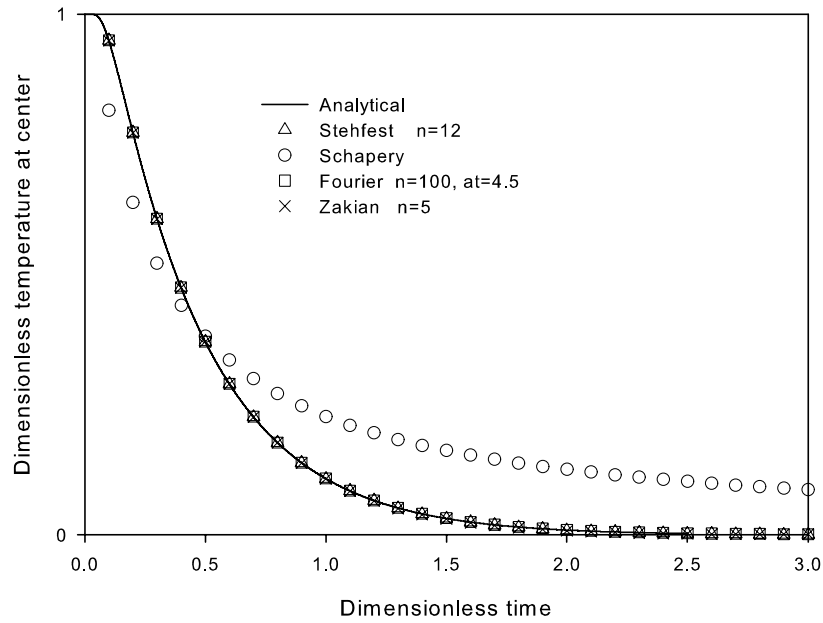


Fig. 13. Comparison of different numerical inversion methods for heat conduction.

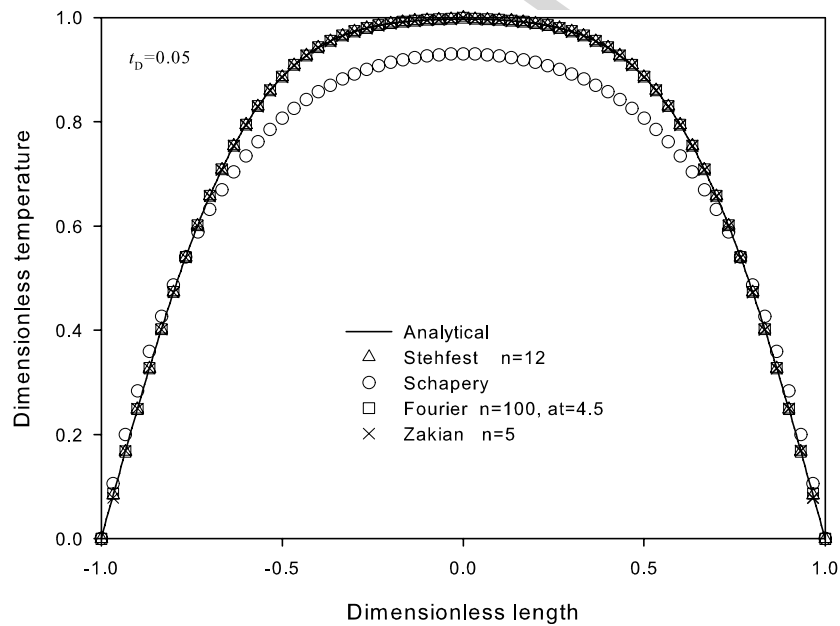


Fig. 14. Comparison of different numerical inversion methods for heat conduction.

6.12. Two-stage reactor

A simple model of a two-stage reactor with recycle is chosen in this part. Taiwo [18] and Taiwo et al. [19] reported the Laplace transform of the controlled concentration response as given below

$$F(s) = \frac{C(s)P(s)}{s[1 + C(s)P(s)]}, \tag{21}$$

where

$$C(s) = \frac{10s + 1}{[0.88(2.5s + 1 - e^{-4s})]},$$

$$P(s) = \frac{k(10s + 1)(7s + 1)e^{-4s}}{(10s + 1)(7s + 1)^2 - k^2(10s + 1)e^{-7.8s} + 0.88(7s + 1)e^{-6s}},$$

and

$$k = 0.968.$$

Functions of this type are known to present problems to Laplace inversion algorithm [19]. This function is inverted by different methods, and the results are compared with the time response reported in by Taiwo et al. [19]. Fig. 15 shows that all the inversion methods except Schapery’s predict values close to the reference solution. The results from Stehfest’s inversion method show small deviations from the reference solutions.

6.13. Non-isothermal gravity drainage of a single matrix block in naturally fractured reservoirs

The test function chosen here is the solution to the non-isothermal gravity drainage of a slab-shaped single matrix block in a naturally fractured reservoir. Thermal oil production from a fractured reservoir involves the injection of steam to warm up the high viscosity oil in the matrix blocks and enable the oil to drain into the fracture system that can be produced. The partial differential equation describing one dimensional heat flow can be expressed as Eq. (22). The assumptions are given by Pooladi-Darvish et al. [20]

$$\frac{\partial^2 T_D}{\partial x_D^2} + N_{Pe} \frac{\partial T_D}{\partial x_D} = \frac{\partial T_D}{\partial t_D}, \tag{22}$$

$$T_D(x, 0) = 0,$$

$$T_D(0, t_D) = 1, \quad \text{and}$$

$$T_D(x_D, t_D) = 0 \quad \text{as } x_D \rightarrow \infty,$$

where T_D is normalized temperature, x_D is dimensionless distance, N_{Pe} is the Peclet number, and t_D is dimensionless time. The analytical solution for this problem when N_{Pe} is constant is given by [20]

$$T_D(x_D, t_D) = \frac{1}{2} \left[\operatorname{erfc} \left(\frac{x_D + N_{Pe} t_D}{2\sqrt{t_D}} \right) + e^{-N_{Pe} x_D} \operatorname{erfc} \left(\frac{x_D - N_{Pe} t_D}{2\sqrt{t_D}} \right) \right]. \tag{23}$$

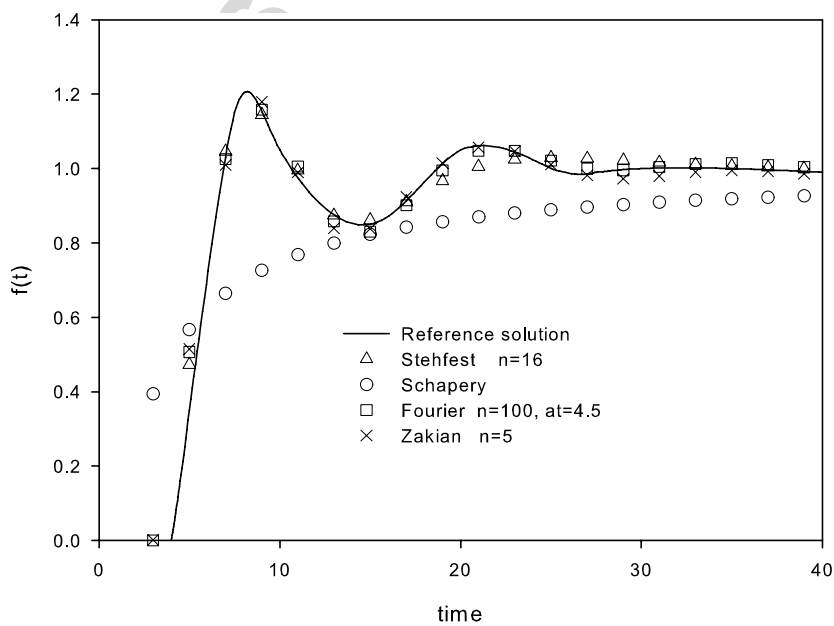


Fig. 15. Comparison of different numerical inversion methods for a two-stage reactor.

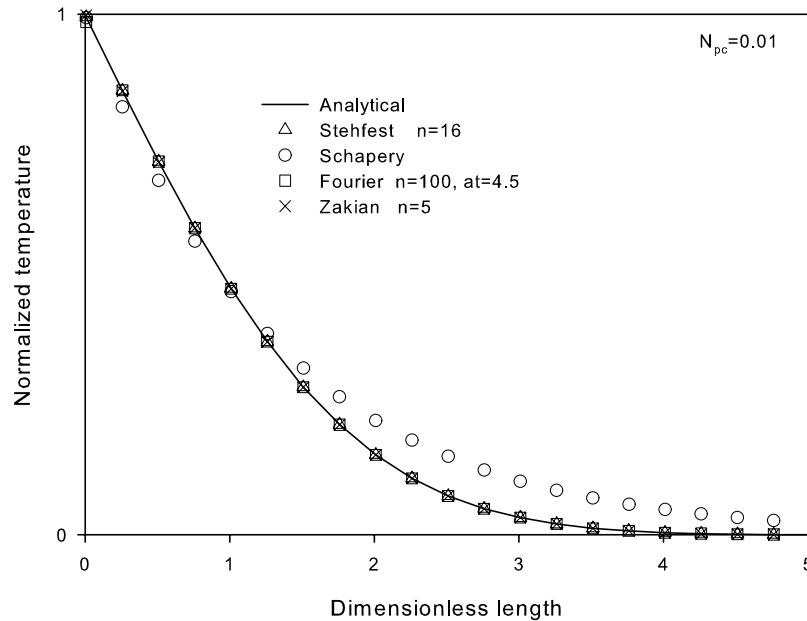


Fig. 16. Comparison of different numerical inversion methods for non-isothermal gravity drainage.

The Laplace domain solution is also given by the following equation:

$$T_D(x_D, s) = \frac{1}{s} \exp \left[-\frac{N_{Pe}}{2} x_D - \left(\sqrt{\left(\frac{N_{Pe}}{2} \right)^2 + s} \right) x_D \right]. \quad (24)$$

This equation is inverted using various methods, and the results are compared in Fig. 16. The results agree well with the analytical solution, except for Schapery's method, which is not accurate.

7. Conclusions

Four Laplace inversion methods were used to evaluate the time domain solution for a variety of problems that arise in engineering applications. In most cases, the results of the inversions compared well with the analytical inversion. Based on the results presented, the following conclusions can be drawn.

- Among all the algorithms tested, the Fourier series technique was the most accurate. It was also found to be applicable to a variety of functions. The disadvantage of this method, however, is that it is difficult to implement and requires a large computation time.
- The Stehfest inversion method is easy to implement. It can be applied to e^{-t} type functions, fractional functions in the Laplace domain, and diffusion problems. However, this method fails to predict e^t type functions or those with an oscillatory response, such as sine and wave functions.
- Results of the Zakian's algorithm are accurate for e^t functions, diffusion problems, and fractional functions in the Laplace domain, which were studied in this paper.
- In the case of functions with oscillatory behaviors, such as Bessel's function of the first kind and the sine function, the results of the Stehfest and Zakian methods are applicable only at early times. Applying these two algorithms gives erroneous results for late time predictions.
- Schapery's method, which is an analytical inversion method, may be used to estimate the global behavior of the solution before applying a numerical inversion method.
- Since numerical Laplace inversion techniques reviewed in this article are not exact, and often depend on the choice of a free parameter that is unknown a priori, it is advantageous to either use more than one inversion technique or perform experimentation and study the effect of the free parameter on the solution.

Acknowledgement

The financial support for this work was provided from Alberta Energy Research Institute (AERI) and NSERC. This support is gratefully acknowledged. The first author also thanks the National Iranian Oil Company (NIOC) for financial support.

References

- [1] M. Abramowitz, I.A. Stegun, *Handbook of Mathematical Functions*, Dover, New York, 1970, p. 1020.
- [2] J.J. Tuma, *Engineering Mathematics Handbook*, McGraw-Hill Company, 1979, p. 214.
- [3] M.R. Spiegel, *Mathematical Handbook of Formulas and Tables*, Schaum's Outline Series in Mathematics, McGraw-Hill Book Company, 1968, p. 161.
- [4] G.P. Gaver Jr., Observing stochastic processes and approximate transform inversions, *Operat. Res.* (1966) 444–459.
- [5] H. Stehfest, Numerical inversion of Laplace transforms algorithm 368, *Commun. ACM* 13 (1) (1979) 47–49.
- [6] S.T. Lee, M.C.H. Chien, W.E., Culham, Vertical single-well pulse testing of a three-layer stratified reservoir, in: *SPE Annual Technical Conference and Exhibition*, 16–19 September, Houston, Texas, 1984, SPE 13249.
- [7] V. Zakian, Numerical inversions of Laplace transforms, *Electron Lett.* (1969) 120–121.
- [8] V. Zakian, Properties of I_{MN} approximants, in: P.R. Graves-Morris (Ed.), *Pade Approximants and Their Applications*, Academic Press, London, 1973, pp. 141–144.
- [9] D.J. Halsted, D.E. Brown, Zakian's technique for inverting Laplace transform, *Chem. Eng. J.* 3 (1972) 312–313.
- [10] H. Dubner, J. Abate, Numerical inversion of Laplace transforms and the finite Fourier transform, *J. ACM* 15 (1) (1968) 115–123.
- [11] R.A. Schapery, Approximate methods of transform inversion for viscoelastic stress analysis, in: *Proc. 4th US Nat. Congr. Appl. Mech.*, 1962, pp. 1075–1085.
- [12] T.A. Jelmert, The effect of distributed block length function on double porosity transitions during linear flow, *J. Petrol. Sci. Eng.* 12 (1995) 277–293.
- [13] F. Veillon, Numerical inversion of Laplace transform [D5], *Collected Algorithms from CACM*, Algorithm 486 (1972) 587–589.
- [14] N. Kitahara, D. Nagahara, H. Yano, A numerical inversion of Laplace transform and its application, *Franklin Inst. J.* (1988) 221–233.
- [15] A.S. Odeh, D.K. Babu, Comparison of solutions of the nonlinear and linearized diffusion equations SPER, 1998, pp. 1202–1206.
- [16] F. Firoozabadi, K. Ishimoto, Reinfiltration in fractured porous media: part I –one dimensional model, *SPE Adv. Technol. Ser.* 2 (2) (1991) 35–44.
- [17] M.A. Sabet, *Well Test Analysis*, Gulf Professional Publishing Company, Houston, TX, 1991.
- [18] O. Taiwo, Controlling plants with recycle, in: *Second European Control Conf.*, Groningen, The Netherlands, 1993, pp. 7–12.
- [19] O. Taiwo, J. Schultz, V. Kerbs, A comparison of two methods for the numerical inversion of Laplace transforms, *Comput. Chem. Eng.* 19 (3) (1995) 303–308.
- [20] M. Pooladi-Darvish, W.S. Tortike, and S.M. Farouq Ali, Steam heating of fractured formations containing heavy oil: basic premises and a single-block analytical model, in: *SPE Annual Technical Conference and Exhibition*, 25–28 September, New Orleans, Louisiana, 1994, SPE 28642.